

## A THEOREM FOR OPTIMUM FINITE-ELEMENT IDEALIZATIONS†

W. E. CARROLL

Department of Engineering Mechanics and Materials Sciences,  
Florida Technological University, Orlando, Florida

and

R. M. BARKER

Department of Civil Engineering, Virginia Polytechnic Institute and State University,  
Blacksburg, Virginia 24061

**Abstract**—A development is presented which serves to characterize the nature of an optimum finite-element idealization. It is shown, utilizing the displacement formulation, that a true minimum of the system potential energy must consider the idealization geometry as a primary parameter. As a consequence, two optimization equations result, one the usual equilibrium equation and the other a residual equation involving gradients of the stiffness matrix and load vector resulting from changes in the idealization. A technique for determining the optimum solution is described and is applied to an elementary two-dimensional example. Practical recommendations are given based on an examination of the residuals associated with the optimization process.

### 1. INTRODUCTION

AS SHOWN by Melosh [1], the finite-element technique can be cast into the framework of an extremum principle by formulating the potential energy of the system under investigation. Such a formulation not only allows the examination of the system in its most elementary form, but also allows, as indicated by Carroll [2] and Marcal [3], the inclusion of the geometry of the idealization as unknown parameters. In this section the necessary arguments will be given for including the idealization geometry as unknowns in the problem. The formulation will be limited to linear elastic materials, but it seems reasonable that similar statements will be valid for more general cases of material behavior.

To introduce the concept of including the idealization geometry as a variable in the potential energy, it is necessary to examine how the element stiffness matrix is formed. This matrix is given in local coordinates by the expression

$$[K]^e = \int_0^{l_1} \int_0^{l_2} \int_0^{l_3} [B]^T [D] [B] d\xi d\eta d\zeta \quad (1.1)$$

where the limits of integration  $l_k$  represent the lengths of the element in the three local coordinate directions as shown in Fig. 1. Thus, it becomes apparent that the stiffness matrix is dependent on all of these lengths.

† This research has been sponsored by the Department of Defense, U.S. Army, Contract No. DAA-F07-69-C-044 with Watervliet Arsenal, Watervliet, N.Y.

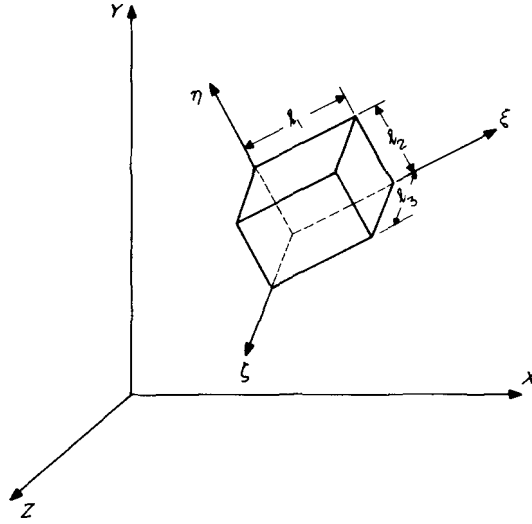


FIG. 1. Idealization geometry for single element in local coordinate system.

For clarity and convenience the local  $\xi, \eta, \zeta$  coordinates will now be chosen to coincide with the global  $x, y, z$  coordinates. Examining Fig. 2 which corresponds to a subdivided continuum, it can be seen that each element will have associated with it a set of lengths descriptive of its overall geometry. It can also be seen that the assembled global stiffness matrix  $[K]$  is also dependent on all of these parameters. For the subdivision depicted in Fig. 2, the total stiffness matrix  $[K]$  should be written as a function of the idealization

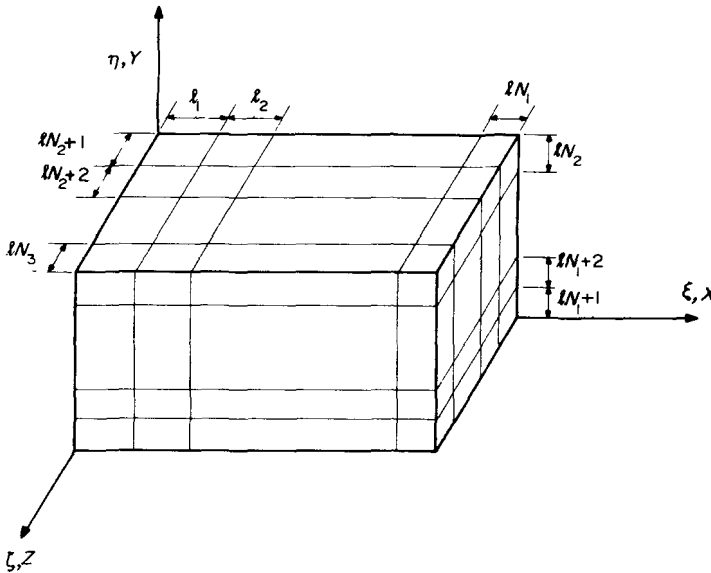


FIG. 2. Idealization geometry for assembled elements in global coordinate system.

parameters of the individual elements, i.e.,

$$\sum_{e=1}^N [K]^e = [K] = [K(l_k)] \quad (1.2)$$

where  $N$  = total number of elements.

In addition, a similar argument applies to the construction of the global load vector  $\{P\}$ . The expression for the local load vector is given as

$$(\{P\}^e)^T = \int^{V^e} \{P_b\}^T [N] dv + \int^{S^e} \{P_s\}^T [N] ds \quad (1.3)$$

and is dependent on the limits of integration which define the volume and surface on which the body and surface forces act. The global load vector is formed by summing up the local values and is, therefore, also dependent on all of the lengths of the elements, i.e.,

$$\sum_{e=1}^N (\{P\}^e)^T = \{P\}^T = \{P(l_k)\}^T. \quad (1.4)$$

The above arguments, whether applied to the simple rectangular geometry used in Fig. 2 or a more general curvilinear coordinate system, still apply. The net effect is the recognition that the potential energy, in addition to being a function of the unknown global displacement vector  $u_i$ , must also be considered as a function of idealization geometry, i.e.,

$$\pi = \pi(u_i, l_k) \quad (1.5)$$

To produce a true minimum on (1.5), necessitates not only considering the equilibrium equation,

$$\partial\pi/\partial u_i = K_{ij}u_j - P_i = 0 \quad (1.6)$$

but also the following additional equation in  $l_k$ ,

$$\frac{\partial\pi}{\partial l_k} = \frac{1}{2}u_i \frac{\partial K_{ij}}{\partial l_k} u_j - \frac{\partial P_i}{\partial l_k} u_i = r_k = 0 \quad (1.7)$$

subject to the dimensionality constraint that the sum of the  $l_k$ 's in any one coordinate direction must equal the overall length of the assembled structure in that direction. The vector  $r_k$  in (1.7) will be referred to as the residue or residual vector.

It should be mentioned that idealization parameters,  $l_k$ , need not be characterized by a measure of length and that other schemes for labeling these parameters can be used. Perhaps the independent idealization parameters might be more favorably cast into measures of angle and radius as in shell and axisymmetric applications. As long as the necessary relationships between the global stiffness matrix, load vector, and the parameters can be defined, this option is available.

## 2. OPTIMUM FINITE-ELEMENT FORMULATION

In order to prove that by satisfying (1.6) and (1.7) a true minimum is obtained for the total potential energy, the monotonic convergence property of the finite-element method may be employed. A complete discussion of this property is given by Melosh [1] and also

by Key [4]. They indicate the necessary and sufficient conditions which the shape functions must satisfy in order to insure monotonic convergence. Furthermore, they demonstrate that the element used in this paper satisfies the criteria that insures this behavior for successive refinements of the idealization geometry.

In the context of the finite-element method, a refinement of the initial geometry results in a larger number of smaller regions having the same shape as the initial region. Changing element geometry, such as dividing an initially rectangular region into a triangular one, is not an admissible refinement. Acceptable refinements are illustrated in Fig. 3 by dashed lines which indicate the manner in which initial element geometry is maintained during the subdivision process.

By keeping the element shape unchanged, it is possible for the displacements in the refined region to be identical to those in the initial region, and therefore their total potential energies can be identical. Since the minimum potential energy solution is selected for each analysis, the refined region analysis cannot result in a higher total energy solution than that of the initial region, i.e., the process must exhibit monotonic convergence [1].

Based on the above definition of a refinement and the assurance of monotonic convergence, the following theorem is given:

*Theorem*

A necessary consequence of the following refinement sequence

$$\pi_n \geq \pi_{n+1} \geq \pi_{n+2} \cdots \geq \pi_{n+m} \cdots \geq \pi_{\text{exact}} \quad (2.1)$$

where  $m$  represents successive refinements of the initial finite-element mesh  $n$ , is the existence of an optimum sub-division such that

$$\pi_{n+m}(l_i^*) \leq \pi_{n+m}(l_i) \quad (2.2)$$

where  $l_i^*$ 's designate the optimum mesh configuration.

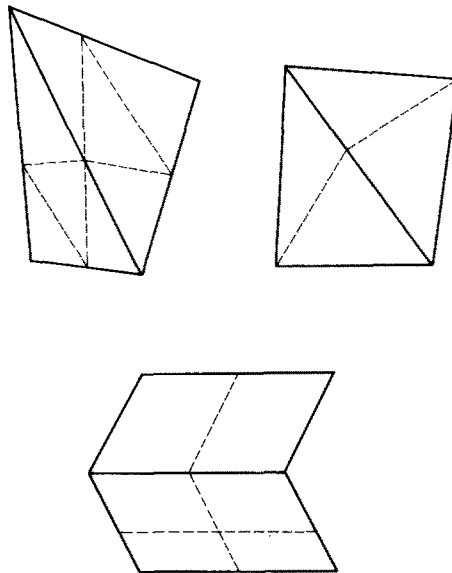


FIG. 3. Admissible finite-element refinements.

*Proof*

Consider the region shown in Fig. 4. Since the dashed line represents a refinement of the initial idealization, whose potential energy will be designated  $\pi_n$ , the following must be true

$$\pi_n \geq \pi_{n+1} \tag{2.3}$$

i.e., the initial idealization constitutes an upper bound on potential energy. Since this equation is in no way dependent upon the position of the refinement, it must hold for all  $l_2$  such that

$$\pi_n \geq \pi_{n+1} \quad \text{for } l_1 \leq l_2 \leq l_3. \tag{2.4}$$

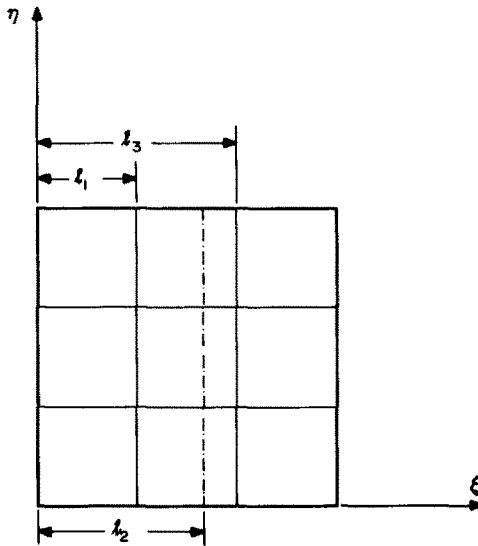


FIG. 4. Refined initial geometry.

The following special cases must also be true if the potential energy is to be continuous and not ill-defined :

$$\pi_{n+1} \rightarrow \pi_n \quad \text{as } l_2 \rightarrow l_1 \tag{2.5}$$

$$\pi_{n+1} \rightarrow \pi_n \quad \text{as } l_2 \rightarrow l_3. \tag{2.6}$$

From the extreme value theorem for a continuous function there must exist an absolute minimum or absolute minimums of equal potential in the interval  $l_1 \leq l_2 \leq l_3$  such that

$$\pi_{n+1}(l_1, l_2, l_3) \leq \pi_{n+1}(l_1, l_2, l_3) \tag{2.7}$$

for which

$$\partial \pi_{n+1} / \partial l_2 |_{i_2} = 0. \tag{2.8}$$

Reapplication of this scheme to successive refinements is possible and by an inductive argument there must exist either a unique set of  $l_i^*$ 's or, for the worst case, multivalued

but equivalent set of  $l_i^*$ 's such that

$$\pi_{n+m}(l_i^*) \leq \pi_{n+m}(l_i) \quad (2.9)$$

where

$$\partial \pi_{n+m} / \partial l_i |_{l_i^*} = 0. \quad (2.10)$$

As already indicated, the solution of equation (2.10) does not guarantee uniqueness. However, it does guarantee the existence, if not unique, of some set of  $L_i$ 's such that the following is true

$$\pi_{n+m}(l_i^*) \leq \pi_{n+m}(L_i) \leq \pi_{n+m}(l_i) \quad (2.11)$$

where

$$\partial \pi_{n+m} / \partial l_i |_{L_i} = 0. \quad (2.12)$$

Sufficiency is only possible if suitable precaution is exercised in the search routine to ensure detection of  $L_i$ 's that are not local maximums or points of inflection.

It should be emphasized that the above proof is general, although limited to the type of subdivisions which satisfy equation (2.2). For problems in which the idealization parameter,  $l_2$ , is not as obvious as in the case of rectangular geometry, additional consideration must be given to the nature of the relationship between the "parent" element and its corresponding counterpart in the transformed space. For example, in using the isoparametric element family the shape function would be used to generate the refined subdivision in the transformed coordinate system.

For the corollaries that follow the existence of (2.11) is adequate. A comparison of (2.12) with (1.7) and the original theorem reveals the following to be true:

*Corollary 1.* A necessary condition for a true minimum on potential energy and for an optimum subdivision to exist for any fixed number of finite elements, in addition to the satisfaction of the equilibrium equation (1.6), is the *vanishing of the residual vector*  $r_k$ .

*Corollary 2.* A necessary condition for convergence to the exact solution of any finite-element refinement sequence is the solution of the optimum subdivision geometry.

*Corollary 3.* The residual vector  $r_k$  must identically vanish if the finite-element solution is exact.

These corollaries will be useful in determining when a finite-element solution has converged to the best possible solution for a given number of elements. Application of the theorem and corollaries to an example problem will be given after a brief discussion of the solution procedure is presented.

### 3. OUTLINE OF SOLUTION PROCEDURE

The solution of equations (1.6) and (1.7) developed in Section 2 cannot be carried out explicitly due to the nonlinear manner in which the parameters  $l_k$  enter into (1.7). In order to satisfy both equations an iterative technique was adopted which consisted of four basic steps. The main features of the solution are summarized in the flow chart of Fig. 5 and outlined in the following paragraphs.

(1) A standard Gaussian elimination scheme is used to satisfy the equilibrium equation (1.6) for an initial guess at the parameters  $l_k$ . The input for this step was often an equidistant spacing of elements but it could be any reasonable idealization geometry.

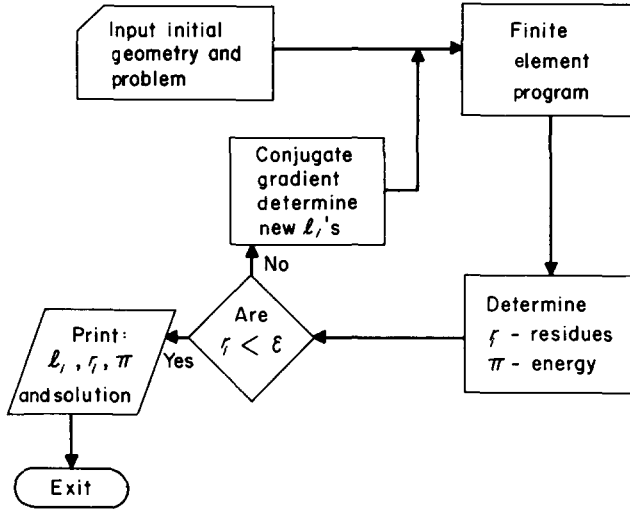


FIG. 5. Solution procedure including idealization geometry.

(2) The residual vector  $r_k$  remaining from (1.7) is determined utilizing the displacements found from the above step. This procedure is easily performed from the computational standpoint as the needed derivatives of the stiffness matrix are stored on a peripheral device as the matrix  $K_{ij}$  is being formed. In a like manner the formulation of the loading vector derivative  $\partial P_i / \partial l_k$  is obtained.

(3) A gradient search method is used for determining a new set of  $l_k$ 's. The gradient technique adopted was one by Fletcher and Reeves [5] which also includes a linear search routine to speed convergence. This routine can be applied to the solution of determining the unconstrained minimum of  $N$  variables. Although the selection of possible  $l_k$ 's is limited by the dimensionality constraint, it was found that as long as the initial iteration was started with  $l_k$ 's defined by points in the problem subspace, few difficulties were encountered.

(4) The residual vectors  $r_k$  for each subsequent iteration are monitored until they fall below some prescribed value or vanish. When they satisfy the given tolerance, the optimization routine is terminated and the final values of  $\pi$ ,  $l_k$  and  $r_k$  are printed as a solution to the problem.

#### 4. ELEMENT SELECTION AND PROBLEM FORMULATION

Application of the idealization technique is now demonstrated for problems in which the finite-element solution is performed by employing two dimensional elements. Numerical examples are limited to application of the rectangular 8-DOF element shown in Fig. 6, whose displacement function can be written in terms of the local coordinates as

$$u_\xi = \alpha_1 \xi + \alpha_2 \xi \eta + \alpha_3 \eta + \alpha_4 \tag{4.1a}$$

$$u_\eta = \alpha_5 \xi + \alpha_6 \xi \eta + \alpha_7 \eta + \alpha_8 \tag{4.1b}$$

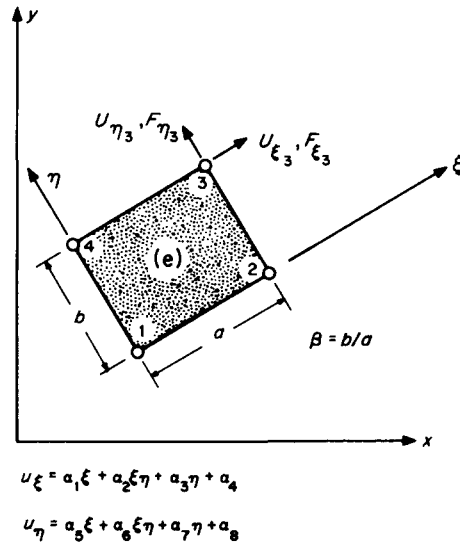


FIG. 6. Rectangular 8-DOF finite-element in local coordinates.

where  $\xi$  and  $\eta$  are length measures in the local coordinate system and the  $a_i$ 's are the generalized coordinates. In these examples, for simplicity, the local coordinate system designated  $\xi, \eta, \zeta$  will be selected to coincide with the global  $x, y, z$  axes.

Primary in the selection of this element for the investigation was the explicit manner in which the stiffness matrix  $K_{ij}$  is expressible in terms of the idealization parameters,  $l_i$ 's, and the ease with which  $K_{ij}$  can be manipulated in order to arrive at a suitable substitution into equation (1.7). For detail on the manner in which the necessary relationships are determined in order to arrive at a suitable substitution into equation (1.7), the reader is referred to Carroll [2].

Referring to Figs. 7-9 the basic problem posed is to determine, given the number of elements shown, the optimum arrangement of these elements to minimize the system potential energy under the following loading conditions:

1. Cantilevered beam—concentrated end moment (Fig. 7)
2. Cantilevered beam—concentrated shear load (Fig. 8)
3. Cantilevered beam—uniformly distributed load (Fig. 9).

These three loadings represent cases for which exact displacements require successively higher powers in the coordinate  $x$ . It should be noted that for these initial results no optimization was considered or found necessary in the global  $y$ -direction, due to the inherent symmetry of the problems under investigation. In all cases the  $y$ -residue vector was calculated and found to be at a level associated with truncation error of the IBM 360 used. For Load Case 3 the distributed load was applied at the neutral axis.

The output of this series is presented graphically in Figs. 7-9 and serves to indicate the beam configuration before and after optimization, the potential energy at these two states, and results for stresses and displacements. It can be seen from this series that more drastic improvement in solution is possible as the mismatch becomes greater between the exact solution displacements and the finite element piecewise linear representation.



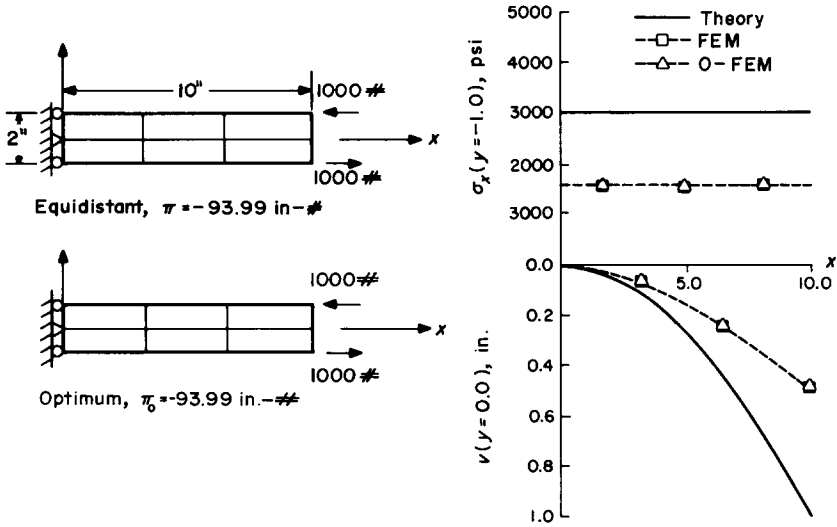


FIG. 7. Comparison of equidistant and optimum finite element solutions for concentrated end moment ( $2 \times 3$  mesh).

For example, Load Case 1 has as its optimum idealization geometry the equidistant assumed mesh. The exact displacements are of order  $x^2$  and thus this load case represents what will be termed a first order mismatch between exact solution displacements and the finite element representation. Although this satisfies the Corollaries concerning convergence given in the previous section, these are, of course, only necessary conditions and it can be shown, by refining this mesh further, minimization is achieved. It has been the author's experience that the optimum idealization geometry is characterized by an equidistant mesh whenever a first order mismatch occurs.

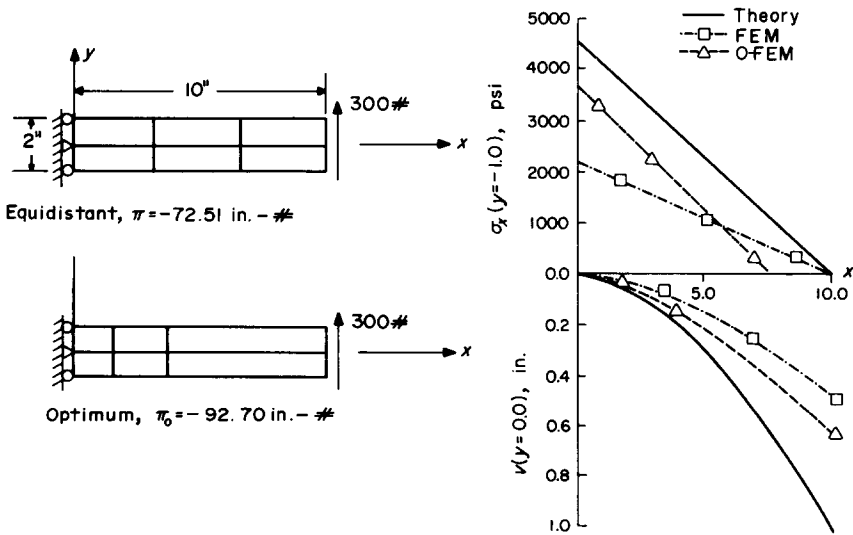


FIG. 8. Comparison of equidistant and optimum finite-element solutions for shear end load ( $2 \times 3$  mesh).

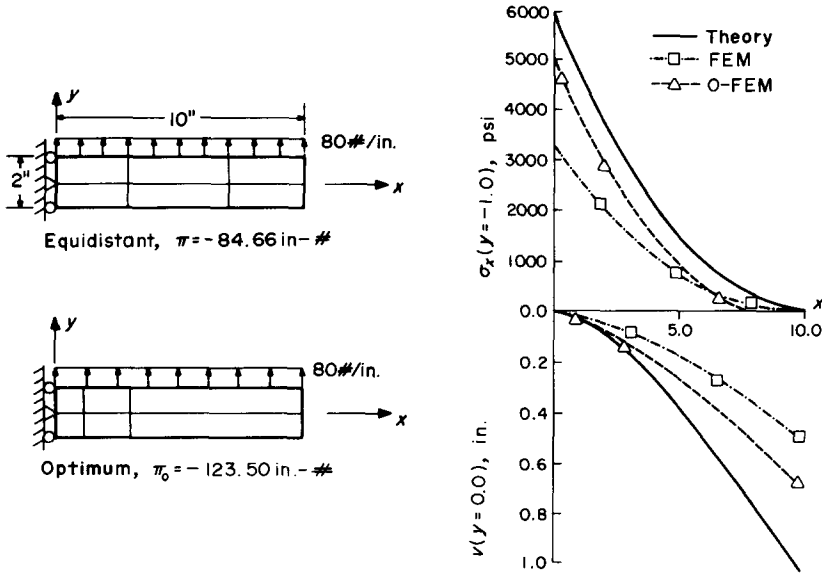


FIG. 9. Comparison of equidistant and optimum finite-element solutions for uniform load (2 x 3 mesh).

This observation has practical implications concerning the manner in which comparison between elements having different displacement functions are performed.

The authors cite an example by Doherty *et al.* [6] in which they examined the same series of problems presented in this paper. There a 10-DOF element, labeled Q5 utilizing the displacement function and geometry shown in Fig. 10, was compared to the 8-DOF generalized quadrilateral element, labeled Q4, also shown in the figure. For rectangular boundaries the Q4 element reduces to the familiar 8DOF rectangular element used throughout this section. Comparing the result presented in Table 2 from their analyses reveals that when the Q5 element is compared with the optimum Q4 arrangement, labeled O-Q4, only a marginal improvement is noted. Based on this argument there seems no justification for concluding the Q5 element superior to the Q4 for this problem sequence. Since the Q5 element results are, of course, non-optimum, it is difficult to determine which element has the "potential" for determining the best solution. But it would appear that from a solution standpoint, convergence studies directed at demonstrating the superiority of improved elements based on identical mesh configurations need reevaluation.

In addition to these results, the summary given in Table 1 serves to indicate the effect on computer time as more refined mesh configurations are employed. Here a balance between economic considerations and solution improvement must be weighed. In general, dramatic improvements in finite-element solution is possible for very coarse mesh configurations with a reasonable increase in computer time. However, as mesh subdivisions become finer, or as more elements are utilized in the discretization process, the adverse effects of solving the non-linear equations that result from employing equation (1.7) becomes apparent. For these finer mesh configurations the actual magnitude of the improved solution also becomes marginal and this suggests a monitoring of the residual vectors, the largest of which is shown in this table, as an indication of when convergence has been achieved.

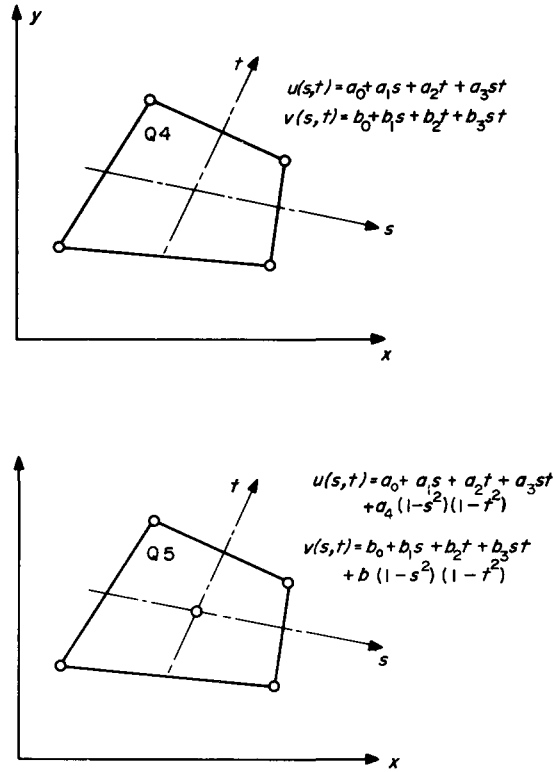


FIG. 10. Four and five node generalized quadrilateral elements.

TABLE I. SUMMARY STATISTICS FOR SHEAR END LOAD CANTILEVERED BEAM

DOF (Mesh)	Idealization	Potential energy	Tip deflection	$\sigma_{max}$ ( $y = -1.0$ in)	Largest residue	CPU Time (relative)
12 (2 × 3)	Equidistant	- 72.51 in-#	0.483 in	2150 psi	14.7	—
	Optimum	- 92.70 in-#	0.618 in	3550 psi	< 0.0001	
18 (2 × 5)	Equidistant	- 108.97 in-#	0.726 in	3250 psi	14.4	—
	Optimum	- 121.67 in-#	0.811 in	4150 psi	< 0.0001	
24 (2 × 7)	Equidistant	- 126.49 in-#	0.843 in	3800 psi	10.7	—
	Optimum	- 134.25 in-#	0.895 in	4300 psi	< 0.0001	
30 (2 × 9)	Equidistant	- 135.46 in-#	0.902 in	4050 psi	7.7	1.5
	Optimum	- 140.54 in-#	0.936 in	4400 psi	< 0.0001	
36 (2 × 11)	Equidistant	- 140.51 in-#	0.936 in	4400 psi	5.7	2.2
	Optimum	- 144.05 in-#	0.960 in	4450 psi	< 0.0001	
42 (2 × 13)	Equidistant	- 143.59 in-#	0.957 in	4500 psi	4.4	2.7
	Optimum	- 146.19 in-#	0.974 in	4500 psi	< 0.0001	
48 (2 × 15)	Equidistant	- 145.59 in-#	0.970 in	4500 psi	3.4	4.0
	Optimum	- 147.68 in-#	0.983 in	4500 psi	< 0.0001	
	Theory	- 154.50 in-#	1.030 in	4500 psi		

TABLE 2. COMPARISON OF OPTIMUM FINITE-ELEMENT RESULTS WITH REF. [6]\*

End moment—Displacements $v$ at $y = 0$ ( $2 \times 5$ mesh)						
	$x$	2	4	6	8	10
Finite element	Q4	2.82	11.29	25.41	45.17	70.58
	Q5	3.02	12.10	27.24	48.43	75.67
	O-Q4	2.82	11.29	25.41	45.17	70.58
Theory		4.00	16.00	36.00	64.00	103.00
Shear load—Displacements $v$ at $y = 0$ ( $2 \times 5$ mesh)						
	$x$	2	4	6	8	10
Finite element	Q4	4.39	15.51	31.74	51.34	72.65
	Q5	4.67	16.51	33.92	54.90	77.71
	O-Q4	5.80	18.90	38.80	59.40	81.11
Theory		6.20	22.00	45.00	77.80	103.00
Uniform load—Displacements $v$ at $y = 0$ ( $2 \times 5$ mesh)						
	$x$	2	4	6	8	10
Finite element	Q4	6.03	19.11	36.22	55.07	74.30
	Q5	6.38	20.34	38.64	58.82	79.43
	O-Q4	7.60	24.90	45.60	66.10	86.00
Theory		8.42	26.88	50.88	77.23	104.00

\* All data based on  $E = 1500.0$  psi.

## 5. CONCLUSIONS

In examining the results for the problems presented, a general overall improvement in displacements is noted when comparison is made with exact behavior. Indeed, the dependence on the mismatch between the finite-element displacement function and exact displacements seems to suggest the displacement sensitivity of the discretization or idealization process for the displacement formulation.

Based on the numerical studies conducted, several aspects of the technique have immediate application to the finite-element user:

1. For coarse mesh configurations the direct application of this technique is suggested. Here, dramatic improvement in solution is available to the finite-element user with a relatively small increase in computer time. This is expected to have appeal to the three-dimensional finite-element investigator who often is limited, by virtue of available computer storage, to a small number of large degree of freedom elements.

2. For fine mesh configurations for which the direct solution of the optimum geometry is impractical, monitoring of both the potential energy and residual vector  $r_k$  has been shown to provide a clear indication of when convergence has been approached. Although fine meshes preclude the justification of this technique, due primarily to economic considerations, the necessary condition for convergence as given in Corollary (1) still remains.

3. Intuitive approaches often employed in the finite-element discretization process do not adequately describe the manner in which refinements should be made. It is recom-

mended that a "rule of thumb" based upon examining the residue vector  $r_k$  would be more accurate in directing further refinements.

4. Studies directed at demonstrating the superiority of an improved element based on identical mesh configurations need to be reexamined in light of optimum mesh configuration.

5. The question regarding uniqueness still remains. Although indications are that a unique set of  $l_i$ 's was found for each problem solved, there could be problems for which several configurations do exist such that the residue vector  $r_k$  will vanish for some non-minimum set of  $l_i$ 's.

*Acknowledgements*—The authors wish to thank R. P. McNitt and K. L. Reifsnider, Associate Professors of Engineering Mechanics, Virginia Polytechnic Institute and State University, for valuable discussions. The authors are also grateful to the reviewers for their helpful comments and suggestions for improving the paper.

## REFERENCES

- [1] R. J. MELOSH, Development of the Stiffness Method to Define Bounds on Elastic Behaviour of Structures. Ph.D. Thesis, University of Washington, Seattle (1962).
- [2] W. E. CARROLL, On Optimum Idealizations in Discrete Element Analysis. Ph.D. Thesis, Virginia Polytechnic Institute and State University, Blacksburg (1971).
- [3] G. M. MCNEICE and P. V. MARCAL, Optimization of Finite Element Grids Based on Minimum Potential Energy. Technical Report No. 7, Brown University, Providence (1971).
- [4] S. W. KEY, A Convergence Investigation of the Direct Stiffness Method. Ph.D. Thesis, University of Washington, Seattle (1966).
- [5] R. FLETCHER and C. M. REEVES, Function minimization by conjugate gradients. *Computer J.* 7, 2 149 (1964).
- [6] W. P. DOHERTY, E. L. WILSON and R. L. TAYLOR, Stress Analysis of Axi-symmetric Solids using Higher Order Quadrilateral Finite Elements. Structural Engineering Laboratory Report No. SESM 69-3, University of California, Berkeley (1969).

(Received 21 November 1971; revised 2 January 1973)

**Абстракт**—Дается разработка задачи для изображения природы оптимальной идеализации конечного элемента. Указано, пользуясь формулами для перемещений, что точное минимум потенциальной энергии системы должно рассматривать геометрию идеализации, в качестве параметра, имеющего первостепенное значение. В результате, происходят два уравнения оптимизации, первое обыкновенное уравнение равновесия и другое остаточное уравнение, заключающее градиенты матрицы коэффициентов жесткости и вектор нагрузки, вследствие изменений в идеализации. Описывается метод для определения оптимального решения и применяется к расчету элементарного, двухразмерного примера. Даются полезные указания на основе исследования вычетов, связанных с процессом оптимизации.